

Evaluation of ice detecting sensors by icing wind tunnel test

Prof. S. Kimura^{*1}, Dr. T. Sato^{*2}, Prof. Y. Yamagishi^{*1} and H. Morikawa^{*3}

^{*1} Kanagawa Institute of Technology

^{*2} National Institute for Earth Science and Disaster Prevention

^{*3} Meteorological Research Institute for Engineering Co.

1030 Shimo-Ogino Atsugi, Kanagawa, Japan 243-0292, skimura@me.kanagawa-it.ac.jp

Abstract—In order to establish an approach for forecasting atmospheric icing events, it is important to acquire data from field observations and create databases for verifying its accuracy. Further, acquisition of accurate data about icing events is of great importance in itself from the meteorological point of view. The sensor used to detect icing is called ice detector. Although ice detectors have been widely used for ensuring safe operation of aircrafts, detectors that can be used for long-term and automated observations of atmospheric icing on structures on the ground have not been frequently used. In this study, icing wind tunnel tests were conducted as a part of a research campaign undertaken by the European Cooperation in Science and Technology (COST) Action 727 for evaluating the performance of ice detectors. In the icing wind tunnel tests, four ice detectors, including two commercially available ice detectors, selected by the Action 727 for field measurements were tested. Because of the limitations of icing wind tunnel tests, only the fundamental characteristics of the detectors were examined under constant icing conditions. The test results indicated that all the target detectors functioned satisfactorily under light icing conditions or when they were exposed to an icing environment only for a short period. Further improvements are required for more stable and reliable field measurements involving long-term observations.

I. INTRODUCTION

An ice detector is a sensor that can detect icing events. Although icing may sometimes lead to serious accidents that cause damage to the social infrastructure, icing events are not regularly monitored by standard weather observations, even in areas prone to icing. Generally, the occurrence of icing events is predicted by using meteorological data such as temperature, wind speed, precipitation, and/or visibility if ice detectors cannot be used directly. The rapid progress in the techniques used for numerical weather forecasting has led to the development of a numerical model for forecasting atmospheric icing. This model can be verified by comparing its results with the data obtained by monitoring icing events. Germany and the Czech Republic have been collecting data of icing events at two stations where the ice load is measured manually [1,2]. However, except for these two stations, icing data has not been collected continuously as a part of meteorological observations. Therefore, accurate and reliable ice detectors have to be developed in order to develop an automated system for icing data acquisition, which can be used in stations located in remote areas. As a part of the campaign

undertaken by the European Cooperation in Science and Technology (COST) Action 727 that was established for developing a new approach for forecasting atmospheric icing events and measuring icing data, icing wind tunnel tests were conducted for evaluating and validating the present ice detectors.

II. ICE DETECTORS

In the present icing wind tunnel tests, four ice detectors were tested. The specifications of each ice detector are briefly given as follows.

1. Combitech IceMonitor

Combitech (Saab Security at present) IceMonitor (abbreviated as COIM) is the only ice detector designed and manufactured in accordance with the ISO 12494 standard [3]. Therefore, this detector was selected for detecting icing events at the stations selected by COST Action 727. COIM consists of two major parts: a detection rod (50 cm in length and 3 cm in diameter), which is used to collect ice, a casing, which contains a balance to measure the weight of collected ice and a heating system (Fig.1). The detection rod can freely rotate around the longitudinal axis due to the drag force acting on ice deposits. The mechanism of ice detection is quite simple. Under icing conditions, ice accretes on the detection rod and the balance measures the weight of the accreted ice. Since the signal from the balance is transmitted continuously, the icing intensity can be calculated by differentiating the weight of ice with respect to time.

2. Rosemount/BF Goodrich 0871LH1

Rosemount/BF Goodrich 0871LH1 (RMBF), shown in Fig.2, is an ice sensor that is widely used in aircrafts. It has a 1-in-long cylindrical probe with a diameter of 0.25 in, which constantly vibrates longitudinally at 40 kHz. When ice accretes on the probe, the vibration frequencies change due to the increase in mass. The sensor detects this change and transmits a binary signal (0 or 1), from which we can determine whether the icing condition has been attained or not. Soon after detecting ice, the heater is switched on to melt the ice rapidly and then switched off after 5 s. This ice detection cycle is repeated during the operation of the sensor.

3. Hydro-Quebec SYGIVRE

The Canadian company Hydro-Quebec manufactured an ice detector (HQID) by integrating an ice detector probably provided by Rosemount/BF Goodrich. The principle of ice detection and the dimensions of HQID are the same as those of

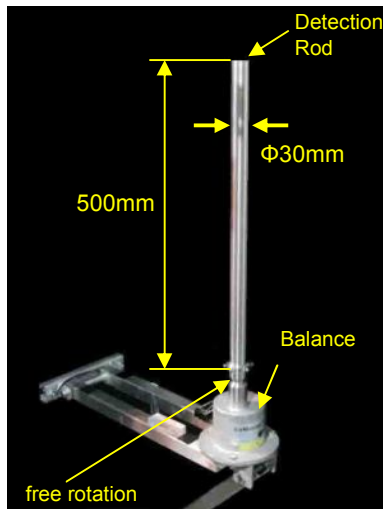


Fig.1 Combitech Icemonitor

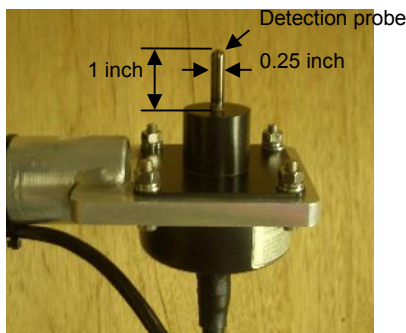


Fig.2 Rosemount/BF Goodrich 0871LH1

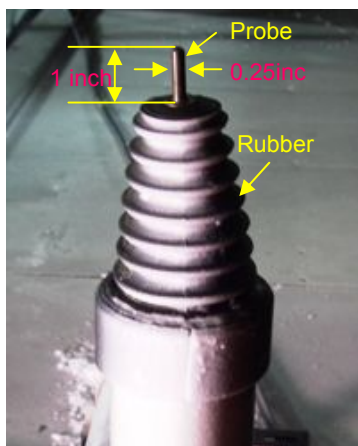


Fig.3 Hydro-Quebec SUGIVRE Ice detector

RMBF. HQID consists of a casing containing a detection device that is covered by a rubber boot, as shown in Fig.3. The unique feature of HQID is that it swings 7 times at an angle of 30° soon after the detection of ice in order to remove the ice or molten water from it head, as shown in Fig.4.

4. HoloOptics T26 Icing Rate Sensor

The HoloOptics T26 Icing Rate Sensor (HO26) was developed by the Swedish manufacturer HoloOptics (Fig.5). A probe emits infrared signals from its tip and receives the signals reflected from the reflector. A heating element is wired behind the reflector in order to melt the ice accreted on the

surface of the reflector. The reflection rate of the reflector varies with the amount of ice formed on the reflector surface, which is the basic principle of detection of ice by this instrument.

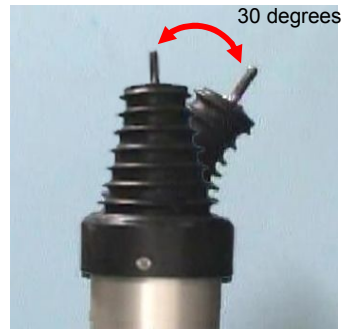


Fig.4 Swing mechanism to remove ice

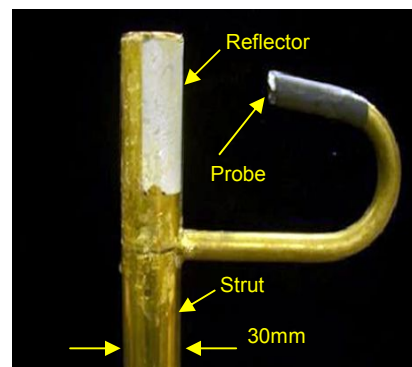


Fig.5 HoloOptics T26 Icing Rate Sensor

III. ICING WIND TUNNEL TEST

1. Test Conditions

As mentioned earlier, the ISO 12494 standard includes the regulations and information regarding detectors to be used for detecting atmospheric icing events. It also specifies a method for icing detection, but does not contain details regarding the tests to be carried out for the evaluation and validation of ice detectors. Thus, the international standard values of the parameters for icing wind tunnel tests are not specified. In the present icing wind tunnel tests, the test conditions were determined as follows. The factors playing an important role in icing wind tunnel tests are the liquid water content (LWC) and droplet size. In the case of clouds, these factors are related to each other as well as to temperature. Various combinations of the LWC and droplet size are shown in Fig.6 [4]. LWC and droplet size were selected to be 0.15–0.7 g/m³ and 20–25 μm, respectively. The air speed and temperature in the wind tunnel test section were set at 12 m/s and -15 °C throughout the tests. In addition, some tests were conducted at room temperature.

2. Icing Wind Tunnel

The icing wind tunnel tests were carried out at two institutes in Japan. One is the National Research Institute for Earth Science and Disaster Prevention, Snow and Ice Research Center, Shinjo Branch, which has a wind tunnel (NIPR-IWT) in the Cryospheric Environment Simulator (CES), as shown in Fig.7. The CES is a large refrigerator and can form artificial

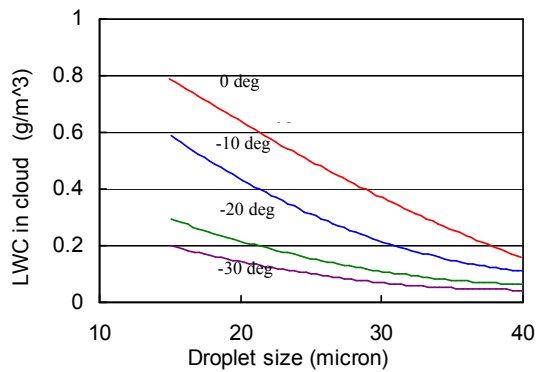


Fig 6. Relation LWC and droplet size[4]

dendritic snowflakes inside it. The cross-sectional area of the wind tunnel test section is 1 m × 1 m. The wind tunnel blockage effect was not taken into account because the projected area of the ice detector was less than 5% of the cross-sectional area of the wind tunnel test section. The maximum speed at the wind tunnel sections is 30 m/s.

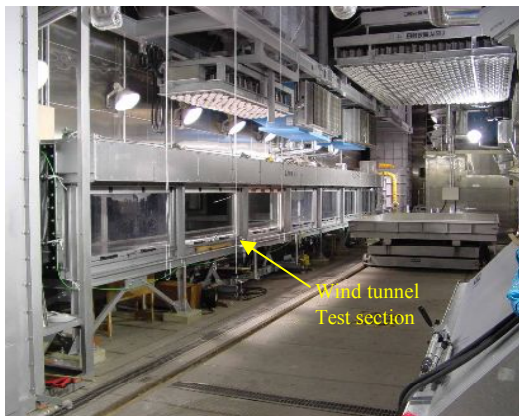


Fig 7. Wind tunnel in the CES of NIED

The other institute where the tests were conducted is the Kanagawa Institute of Technology. It has an Eiffel-type icing wind tunnel (KAIT-IWT), as shown in Fig.8. The wind tunnel has two test sections of different sizes, 100 mm × 300 mm and 500 mm × 500 mm. For icing detection sensors, the larger open-type test section was employed. In such a case, the maximum air speed in the test section is approximately 20 m/s. The temperature can be decreased to -30 °C.

IV. RESULTS AND DISCUSSIONS

1. COIM

The COIM setup in the test section NIPR-IWT is shown in Fig.9. The typical output signal of COIM is shown in Fig.10. In this figure, the line is smoothed by using a moving average procedure using 200 data items. The output strength increases with time, though it fluctuates considerably. As mentioned earlier, the icing intensity is calculated by differentiating the measured weight of ice with respect to time, in this case, the averaged signal. From the results, it is found that a time interval of several minutes, e.g. 10 min, is

necessary for the calculation, although some errors are expected.

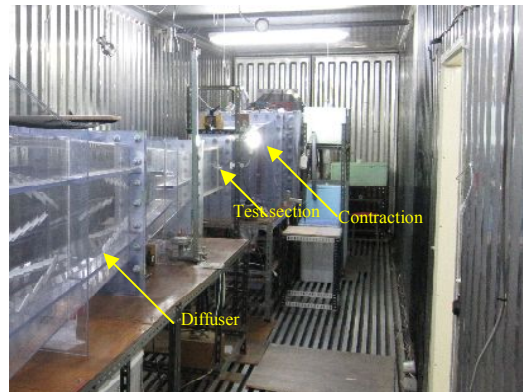


Fig 8. Icing wind tunnel at KAIT



Fig.9 COIM set up in the wind tunnel

The surface status of COIM is shown in Figs. 11(a)–(c). The detection rod of COIM is designed such that that it can rotate freely with wind. However, in the wind tunnel tests, it did not rotate because of the constant air speed in the same direction (during the test, the rod accidentally rotated by approximately 90°). Hence, ice accreted only on the windward side of the rod, as shown in the figures (Fig.11(b)). Moreover, soon after the start of the tests, ice started forming in the connection part between the rod and the casing, although the

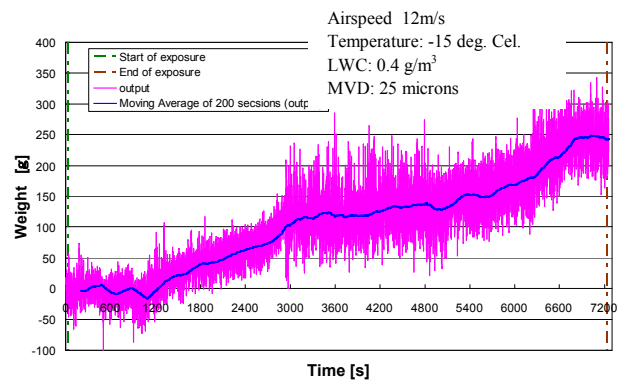
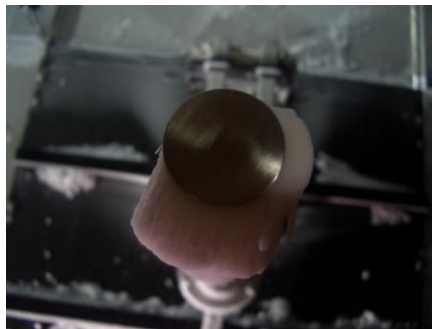


Fig. 10 Output signal from COIM



(a) Full view of COIM



(b) Shape of ice deposit



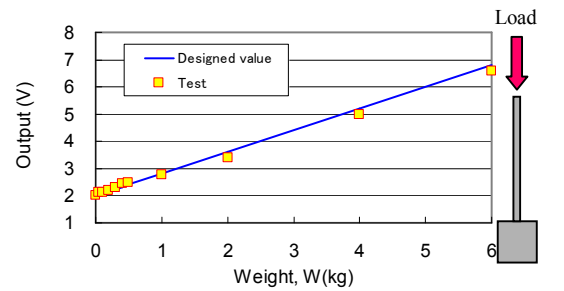
(c) Probe stuck to pedestal

Fig.11 COIM after icing wind tunnel test

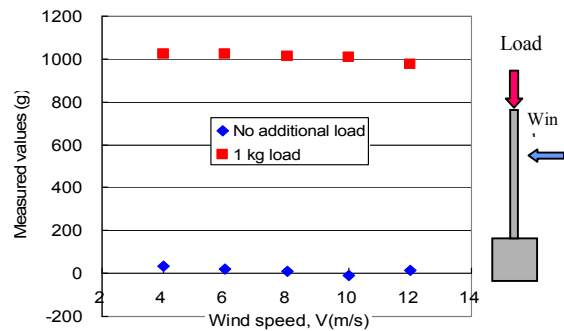
connection part was heated by using an embedded electric heating element, which hampered the probe's rotation and correct weight measurement. This can be avoided by using a heater with higher electric capacity or covering the connection part.

The balance of COIM was tested at room temperature prior to the icing wind tunnel tests. It was tested by applying a longitudinal force under cross air-flow and calm conditions. From Fig.12, it is evident that the balance functioned quite well at room temperature.

Several COIMs were used to detect icing events at several test sites during the campaign undertaken by COST Action 727. They mostly functioned without any problem at all test sites (Fig.13(a)). However, unusual output signals as shown in Fig.13(b) were sometimes reported [5]. Then, another test was conducted in order to evaluate the performance of COIM in a different manner. In the icing wind tunnel tests explained above, COIM was placed in a cold



(a). Test in calm



(b). Test in cross air-stream

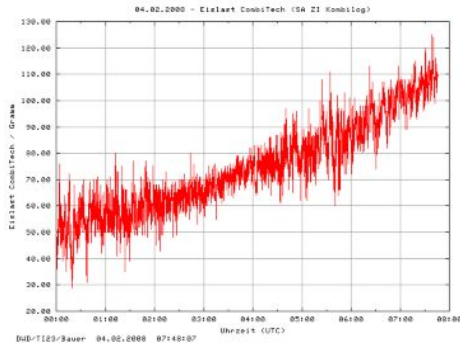
Fig.12 Performance test of the balance

environment for a long time before beginning of the tests, to cool it sufficiently. In the present test, the temperature was gradually decreased from room temperature to $-15\text{ }^{\circ}\text{C}$ with and without the axial force application. The results are shown in Fig.14(a) and (b). As can be seen from these figures, particularly (b), sudden increases are found in the signal. The change in the temperature of the surface of the casing of the balance, indicated by the orange line, shows that the fluctuation of the signal was triggered by the installed electric heater. One possible cause of the fluctuations can be that the load cell of the balance, which is a key component of the balance, might have been affected by the heat from the heater. Another possibility is the electromagnetic noise from the heating element. Unfortunately, we could not find a clear reason behind the fluctuation from the tests.

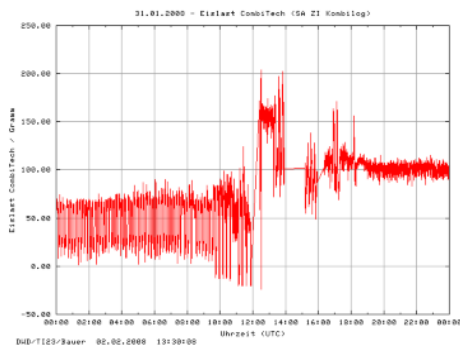
2. RMBF

The ice detection capability of RMBF was examined in KAIT-IWT. Fig.15 shows the RMBF setup in the open-type wind tunnel test section.

The typical pattern of the output signal of RMBF is shown in Fig.16(a) and (b), where the air flow from right to left. At point A, i.e. just after the start of the test, no ice was found on RMBF. At point B, just before detection of icing and switching on the heater, slight accretion of ice on the windward side of the probe and the body of the detector was found. At point C, just after switching off the heater, ice on the probe melted and molten water dribbled to the bottom of the probe. Even with airflow, molten water was not blown off from the surface. At point D, when the transmission of signal of positive detection stopped, ice formed behind the probe due to the congelation of molten water, and the formation of ice on the surface of RMBF continued.



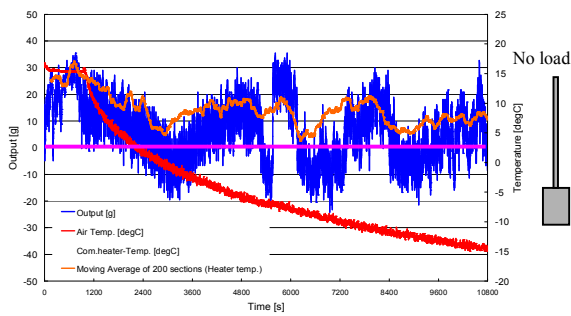
(a). Normal output



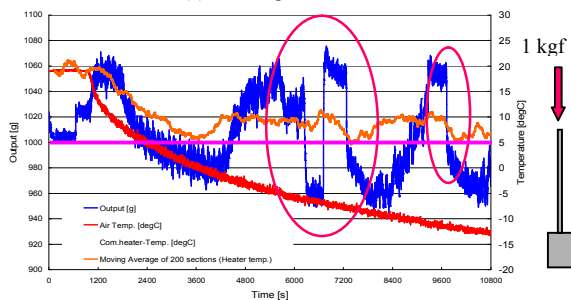
(b). Sudden leap and dive in output

Fig. 13 Examples of the output from COIM Observed in Potsdam, Germany[5]

Courtesy of B. Wichra



(a). No longitudinal force



(b). Applying 1kgf axial force

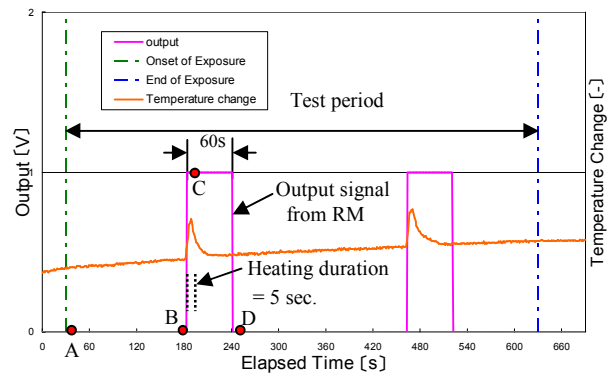
Fig.14 Change of output signals with changing temperature



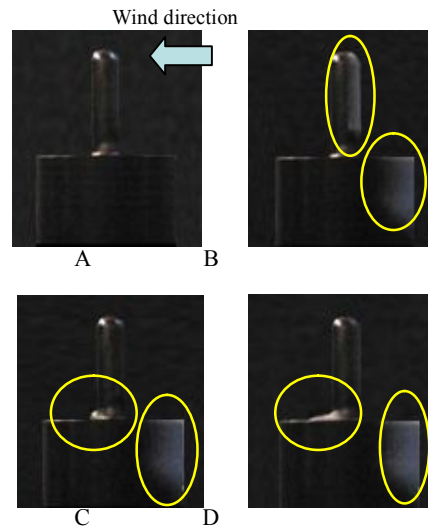
(a). Seen from the leeward

(b). Side view

Fig.15 RMBF set up in the test section



(a). Output signal



(b). Surface conditions

Fig.16 Output signal from RMBF and the surface conditions during the test

Ice collection period (ICP) is defined as the period between the beginning of ice accretion on the probe and the beginning of the detection as indicated in Fig.17. After the heater is switched off, the probe becomes cold due to the cold air flow and simultaneously ice starts collecting on it. In some time, when the mass of the ice accreted on the probe reaches a certain value (0.037 g as described later), the heater is activated. Therefore, ICP would be a measure of the icing

intensity because ICP depends on the air speed, LWC, droplet size, and temperature.

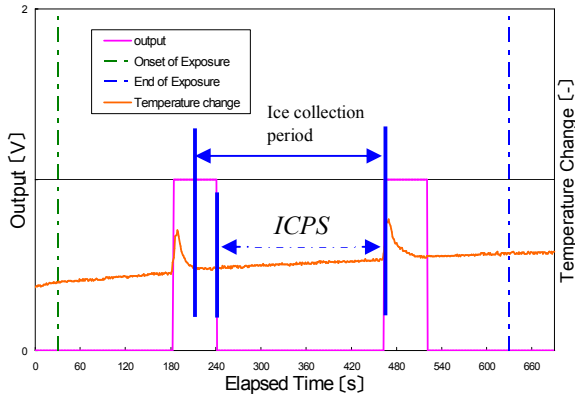


Fig.17 Definition of ice collection period

Additional icing wind tunnel tests were conducted by changing the LWC in order to verify the mass of ice deposits on the probe for the sensor to detect the vibration change. From Fig.18, it is clear that the measured ice masses are distributed around the mean value of 0.037 g in the LWC range of 0.15 and 0.7 g/m³. This indicates that RMBF can detect icing regardless of the icing intensity. This also leads to the confirmation of the premise that the ICP can be used to determine the icing intensity. In fact, ICP decreases almost linearly with the increase in LWC, as shown in the figure. Furthermore, this implies that the ICP tends to be zero in the case of the high icing intensity and, therefore, ice accretion continuously occurs even on the heated probe.

The flow field around RMBF under some condition is shown in Fig.19, where the air flows from left to right. In the circle drawn in the figure, the air flow over the upper corner of the windward side of the detector body passes again over the upper surface of the body along a curved path. Water droplets are also carried by this stream and, hence, some of the droplets may collide with this surface and cause accretion there. As long as RMBF is exposed to icing conditions, this phenomenon continues and ice deposits increase.

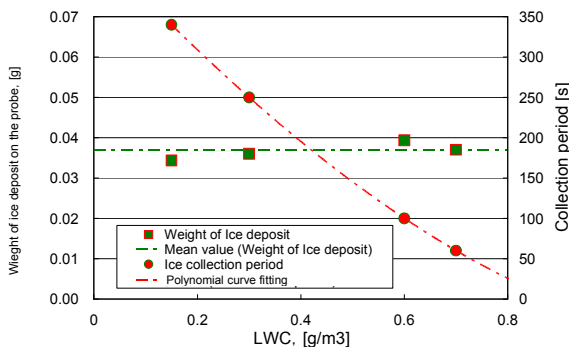


Fig.18 Measured weight of ice deposit on the probe and ice collection period

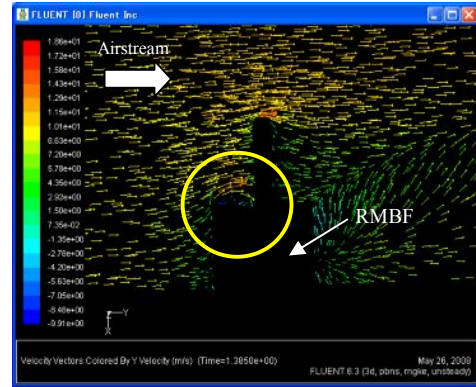


Fig.19 Flow field around Rosemount by CFD

From the abovementioned discussion, we found that there are three types of ice accretions on RMBF:

1. ice formed by the refreezing of molten water at the bottom of the probe,
2. ice formed due to the collision of supercooled water droplets carried by air flow, following a curved path, behind the upper corner of the body,
3. ice accreted on the surface by directly impinged water droplets.

Consequently, it is believed that RMBF would be completely covered with ice after long-term exposure to an icing environment, as shown in Fig.20.

3. HQID

Fig.21 shows HQID in the test section of NIPR-IWT. The principle of ice detection of HQID is the same as that of RMBF. A feature of HQID differentiating it from RMBF is its swing mechanism. This mechanism is used to remove molten water from the probe after detection. As shown in Fig.3, the probe is identical to that of RMBF and mounted on a pedestal with an unheated rubber boot. In Fig.22, the output signal along with the four points A to D are shown. There exist two peaks in the figure. The swinging motion starts soon after the detection. The output appears to be synchronized with this motion, which could have resulted in the two peaks.

The surface status of HQID after the icing wind tunnel test for 20 min is shown in Fig.23. Ice accretes on the rubber boot, on and between the tiers of the boot, which indicates that the swinging motion cannot remove the ice accreted on the rubber boot. As mentioned previously, when an ice detector of this type is placed in an icing environment for a long period of time, ice deposits on an unheated part of the sensor may increase significantly and may finally cover the entire body of the sensor. Hence, HQID may not be useful for long-term measurements.

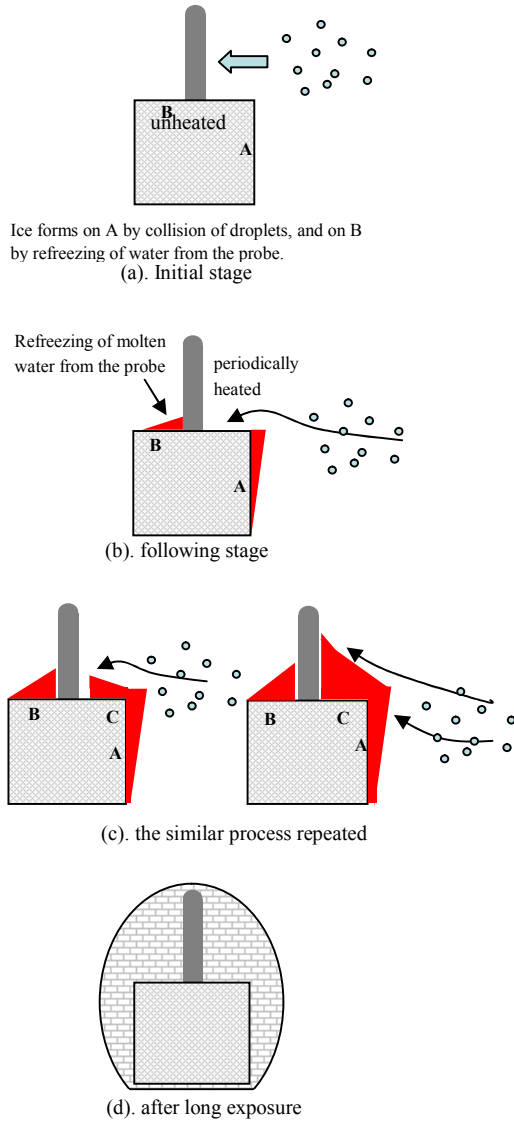


Fig.20 Estimation of ice growth on RMBF after the long exposure to an icing

4. HO26

HO26 placed in the wind tunnel test section is shown in Fig.24. In this setup, the probe of HO26 is directed windward, defined as 0°. The definition of the incident angle is explained in the figure. The detection procedure involves the measurement of the rate of reflection of infrared signals from the reflector. Infrared signals are emitted from the transducer at the tip of the probe and received by the same transducer. Under the prescribed test conditions, HO26 shows the same problem as other detectors simply because of insufficient thermal capacity of the heating element in both the reflector and the transducer.

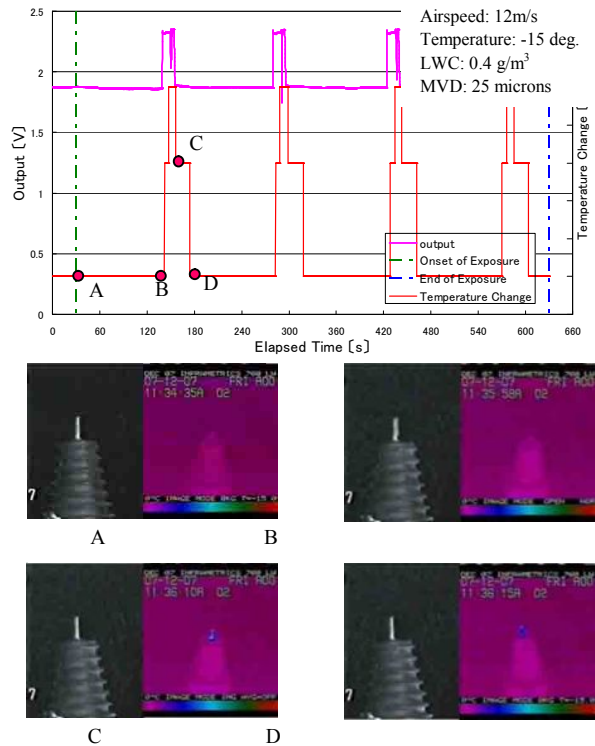


Fig.22 Output from SYGIVRE and temperature of probe

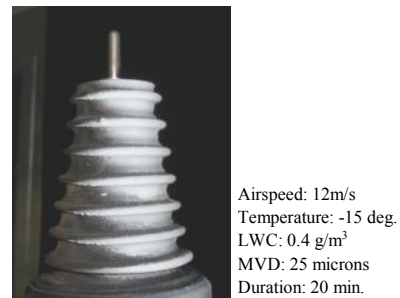


Fig.23 Ice accretion on the rubber boot

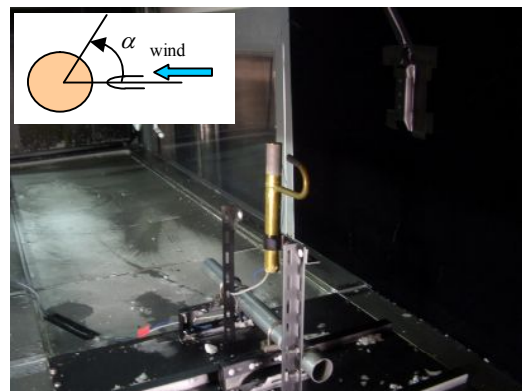


Fig.24 Icing Rate Sensor placed at 0 degree incidence

The output signal and the surface status during the icing detection process of HO26 are shown in Fig.25. As mentioned above, due to the insufficient thermal capacity of the heating element, ice remained on the reflector and the probe. Consequently, HO26 detected ice and transmitted the signal indicating ice detection continuously from the beginning till the end.

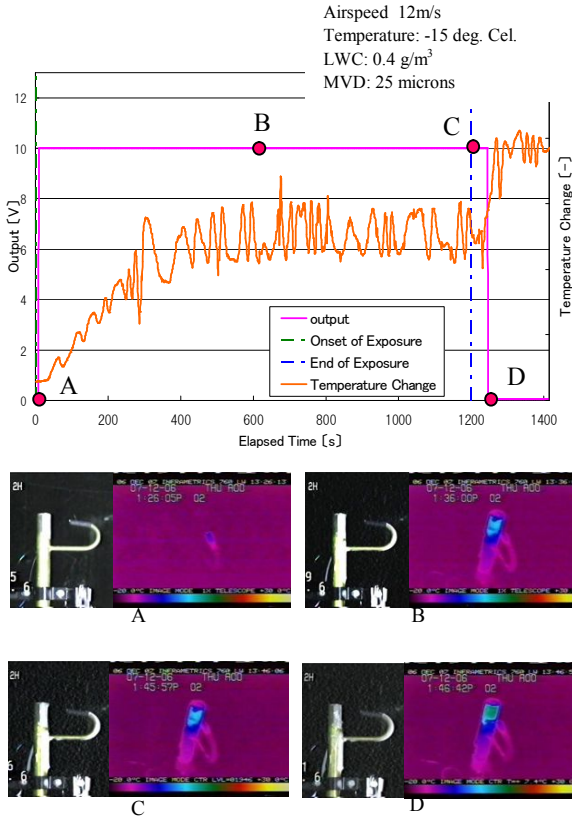


Fig.25 Icing detection process by HOT26

Insufficient of thermal capacity and small heating area caused another problem in the reflector. As shown in Fig.26, an ice bridge connecting the upper and lower edges of reflector was formed. This bridge then covered the reflector and obstructed the incoming infrared signals, resulting in incorrect measurements. Moreover, regardless of the incident angle, ice accreted on every surface of HOT26 in the direction of air flow, as shown in Fig.27.



Fig.26 Ice bridge formed on the reflector

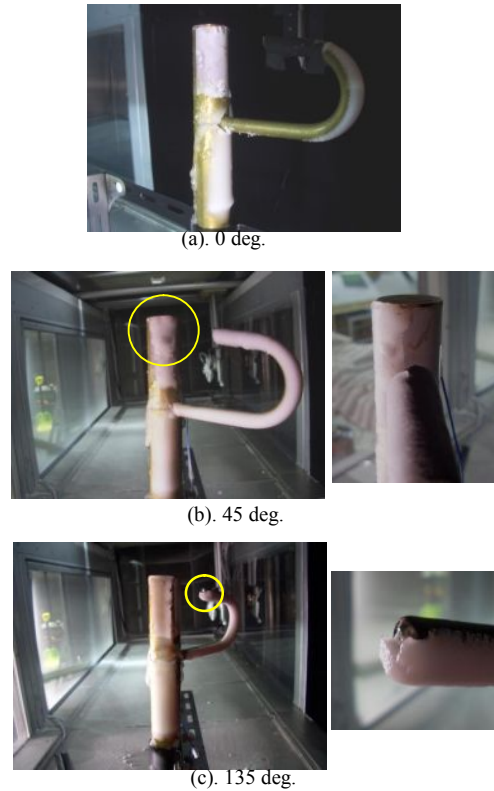


Fig.27 Ice formation at different angles

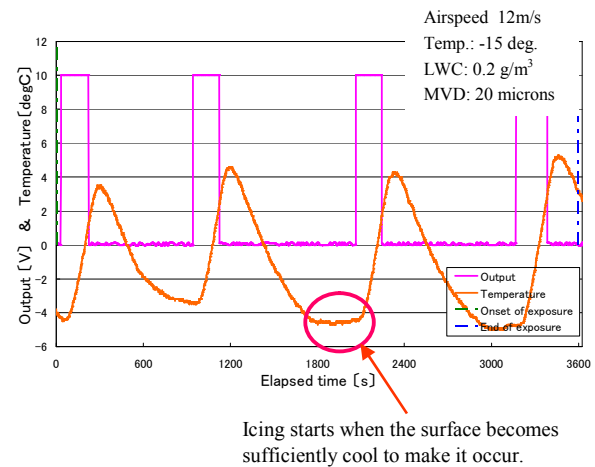


Fig.28 Test in less LWC condition

Under weaker icing conditions with less LWC, HO26 functioned properly as expected, transmitting detection signals intermittently (Fig.28). The sensitivity of this detector is sufficiently high, and therefore, it can be employed under conditions with lower icing intensity.

V. CONCLUSIONS

Icing wind tunnel tests were conducted at the National Research Institute of Earth Science and Disaster Prevention and Kanagawa Institute of Technology for evaluating the fundamental characteristics of ice detectors. The ice detectors

employed for the tests were Combitech (Saab Security at present) IceMonitor (COIM), Rosemount/BF Goodrich 0871LH1 (RMBF), Hydro-Quebec SYGIVRE (HQID), and HoloOptics T26 icing rate sensor (HO26). Following are the findings of our study:

1. RMBF, HQID, and HO26 are quite sensitive to ice accretion and can detect ice soon after it accretes. However, due to the insufficient thermal capacity of the installed heater or the heating element in the ice detecting part and the wide unheated area of the devices, ice deposits may increase when they are exposed to an icing environment for a long time or various conditions such as higher icing intensity, lower temperature, higher wind speed, larger droplet size, or higher water content. In such cases, the sensors cannot detect ice once they are completely covered with ice.
2. RMBF and HQID have the same ice detection mechanism, which is based on sensing the frequency change of the probe caused by the accretion of a certain amount of the ice on the probe. Soon after the detection, the heater is switched on to melt ice, and the detector waits for subsequent signals indicating ice detection. As long as the detectors are exposed to an icing environment, this detection process will be repeated at intervals. Ice collection on the probe depends on the icing intensity such that the interval of ice detections becomes proportional to it. Accordingly, it can be assumed that the icing intensity can be estimated by measuring the detection interval. This type of detection may not be feasible at extremely high icing intensity.
3. HWIQ is designed to swing to remove molten water off the surface and the probe. At temperatures close to the freezing point of water, it may function as expected. But at lower temperatures, a part of molten water from the heated probe comes in contact with the surface of the device and freezes so rapidly that the swinging mechanism cannot remove all water. Moreover, a tiered unheated rubber boot covers the lower part of the device, on which lot of ice is collected. This might lead to increase in ice deposits on the boot, which covers the entire device, when exposed to an icing environment for a short period.
4. Since COIM is designed to measure the weight of ice accreted on the probe up to 10 kg, it could be used throughout the winter regardless of the icing intensity. However, because of its tolerance in measuring the weight of 50 g, icing could not be detected precisely.

Detecting ice accurately and stably during atmospheric icing events, which should be done automatically even in remote areas, must play an important role not only in meteorological prediction but also for disaster prevention. Ice detectors can be used for this purpose. Our study shows that the present ice detectors can be used for measuring atmospheric icing only after slight modification.

VI. ACKNOWLEDGMENT

The ice detectors used in the icing wind tunnel tests were provided by the respective companies and our colleagues. We are grateful to Mr. Per-Erik Persson of Saab Security, Mr.

Rolf Westerlund of HoloOptics, Dr. Alain Heimo of Meteoswiss, and Prof. Noriyoshi Sugarawa of the Kitami Institute of Technology. This study could be completed only because of their kind cooperation.

VII. REFERENCES

Papers from Conference Proceedings (Published):

- [1] B. Wichura, "A Survey of Icing Measurements in Germany", in *Proc. IWAIS XII, Yokohama(CD-ROM), October 2007, 4pages*
- [2] P. Lehky, J. Sabata and L. Zeman, "Observation of Icing on the Stand at Studnice", in *Proc. IWAIS XII, Yokohama(CD-ROM), October 2007, 3pages*

Standards:

- [3] *International Standard ISO12494, Atmospheric Icing*, First Edition, Aug., 2001
- [4] *Federal Aviation Administration, Federal Aviation Regulations, Part 25, Appendix C, Part I- Atmospheric Icing Conditions*

Others:

- [5] B. Wichura: Personal communication. Data collected at Zinnwald station, Germany, 2008